The 2009 IEEE/RSJ International Conference on
Intelligent Robots and Systems
October 11-15, 2009 St. Louis, USA

Analysis of Human-Operated Motions and Trajectory Replanning for Kinematically Redundant Manipulators

Uwe Mettin, Simon Westerberg, Anton S. Shiriaev, Pedro X. La Hera

Abstract— **We consider trajectory planning for kinematically redundant manipulators used on forestry machines. The analysis of recorded data from human operation reveals that the driver does not use the full potential of the machine due to the complexity of the manipulation task. We suggest an optimization procedure that takes advantage of the kinematic redundancy so that time-efficient joint and velocity profiles along the path can be obtained. Differential constraints imposed by the manipulator dynamics are accounted for by employing a phase-plane technique for admissible path timings. Velocity constraints of the individual joints are particularly restrictive in hydraulic manipulators. Our study aims for semi-autonomous schemes that can provide assistance to the operator for executing global motions.**

Index Terms— **Motion Planning, Kinematically Redundant Manipulators, Robotics in Agriculture and Forestry**

I. Introduction

Nowadays most of the harvesting and logging in forestry is performed by human-operated machines. There is a clear trend towards autonomous processes due to the overall benefits from robotics applications in industry [1]. Full automation of forestry machines, however, can be considered as a long-term goal, since serious challenges are addressed regarding motion planning and control of the manipulation tasks, maneuvering through the forest environment, machine perception, localization and mapping. Semi-autonomous schemes, on the other hand, are to be expected in the near future, involving still a human operator but with less complex tasks. For instance, automated motions from start to target points can provide great assistance and stress relaxation to the driver.

We consider the problem of trajectory planning along given Cartesian paths for a hydraulic forwarder crane used to collect logs (see Fig. 1). The human-operated crane is a kinematically redundant manipulator whose end-effector position is controlled in a 4D joint space; its orientation is not controlled. Thus, the movement of the end effector from a start point to an end point is described in a 3D Cartesian space, but its coordination is subject to a higher dimensional configuration space.

Our hypothesis is that the human operator is not able to use the full potential of the machine—even after years of training—due to the complexity of the manipulation task. This investigation is therefore concerned with a smart motion planning strategy for generating efficient end-effector trajectories from given start to end point. The idea is that the driver will still perform local grasping tasks, but gets assistance for executing global motions by automatic control.

Fig. 1. A Valmet Forwarder 860.3 manufactured by Komatsu Forest AB.

Once a desired path is specified in the 3D-world frame, a motion can be planned and executed such that all joints are synchronized and constrained to the Cartesian path. We suggest an optimization procedure that takes advantage of the redundancy from task space to configuration space. Those joint profiles that yield the maximum speed performance along the path are found by employing a phase-plane technique for admissible path timings subject to certain constraints of the mechanical construction and dynamics. Eventually, a time-efficient trajectory along a specified Cartesian path is obtained.

Planning a path at first and then computing a timing function along the path subject to differential constraints is known as *decoupled approach* [5]. We should note that such methods were already introduced in the 1980's by [4], [2], [7] proposing a time scaling of trajectories in order to accommodate actuator torque limitations. The resulting trajectories are time-optimal and require a bang-bang control for switching between accelerating and decelerating at full speed. For hydraulic actuators, however, the apparent velocity constraints are dominant and will therefore be treated carefully in our study.

The rest of the paper is organized as follows. A kinematic model of the crane together with constraints in configu-

The authors are with the Department of Applied Physics and Electronics, Umeå University, SE-901 87 Umeå, Sweden. E-mail: uwe.mettin@tfe.umu.se.

A. Shiriaev is also with the Department of Engineering Cybernetics, Norwegian University of Science and Technology, NO-7491 Trondheim, Norway.

This work is supported by the Center of Intelligent Off-road Vehicles (IFOR) at the Institute of Technology of Umeå University, Komatsu Forest AB, Sveaskog and the Kempe Foundation.

ration and velocities is introduced in Section II. For the analysis of human-operated motions we recorded the process of loading logs and processed this data. Relevant motions for this study are selected in Section III according to the absolute end-effector velocity. In Section IV we analyze a particular human-operated motion in order to illustrate its parameterization without explicit dependence on time. How to replan the trajectory of the operator in order to speed up the motion is shown in Section V as optimization of the velocity profile along the same path, and in Section VI as optimization for finding a time-efficient path. The paper ends with concluding remarks.

II. Modeling the Manipulator

The manipulator used for our study is a typical forwarder crane that is hydraulically powered and consists of a series of links. We are concerned with the manipulation task of moving the end effector from a start point to an end point in the world frame, i.e. local grasping tasks are not considered here. Thus, the robot geometry to be described is an open kinematic chain of four links from the base to the joint where the end effector is attached. The joints are structured as follows:

(0) Base of the robot manipulator.
(1) Revolute joint for *slewing*, associated with q_1.
(2) Revolute joint for the *inner boom*, associated with q_2.
(3) Revolute joint for the *outer boom*, associated with q_3.
(4) Prismatic joint for *telescopic extension of the outer boom*, associated with q_4.
(5) Joint where end effector is attached (*boom tip*).

The joint variables form the vector of generalized coordinates $q = [q_1, q_2, q_3, q_4]^T$ for this 4 degree-of-freedom system.

The forward kinematics can be conveniently expressed using the Denavit-Hartenberg (DH) convention [9], where each link configuration is represented by the homogeneous transformation

$$A_i = \text{Rot}_{z,\theta_i}\,\text{Trans}_{z,d_i}\,\text{Trans}_{x,a_i}\,\text{Rot}_{x,\alpha_i}\,, \qquad (1)$$

parameterized by joint angle θ_i, link offset d_i, link length a_i, and link twist α_i. In Table I the parameters are provided that describe the configuration of the forwarder crane as depicted in Fig. 2.

TABLE I
DH parameters of the 4-link manipulator

Link i	θ_i [rad]	d_i [m]	a_i [m]	α_i [rad]
1	$q_1(t)$	3.24	0.02	$\pi/2$
2	$q_2(t) + \theta_{2,0}$	0	3.40	0
3	$\pi/2 + q_3(t) - \theta_{2,0}$	0	0.21	$\pi/2$
4	0	$d_{4,0} + q_4(t)$	0	$-\pi/2$
Constants: $\theta_{2,0} = 0.0496\,\text{rad}$, $d_{4,0} = 2.42\,\text{m}$				

Eventually, the Cartesian position of the boom tip with respect to the base frame of the robot is defined by

$$p^0 = \begin{bmatrix} x \\ y \\ z \end{bmatrix} = \begin{bmatrix} I_{3\times3} & 0_{3\times1} \end{bmatrix} T_4^0 \begin{bmatrix} 0_{3\times1} \\ 1 \end{bmatrix}, \qquad (2)$$

where $T_4^0 = A_1(q_1)A_2(q_2)A_3(q_3)A_4(q_4)\,.$

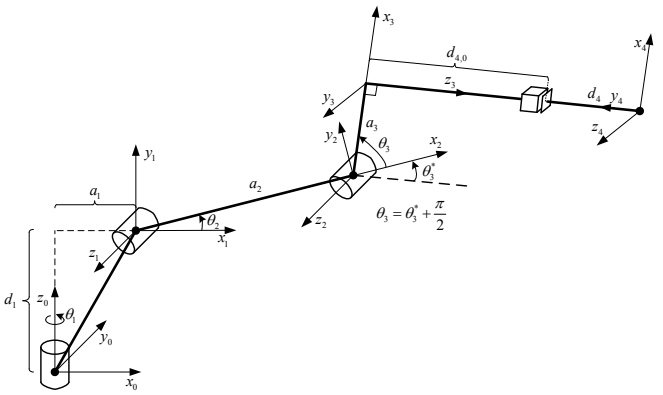

Fig. 2. Configuration of the crane described by the Denavit-Hartenberg convention with parameters given in Table I.

Inverse kinematics from a configuration of the boom tip to the joint variables can be found as a solution of a set of nonlinear trigonometric equations given by T_4^0 in (2). In our case only the boom-tip position shall be specified along some motion such that corresponding joint variables are computed in closed form by a function

$$q = F(p^0, q_4)\,, \qquad (3)$$

where q_4 is the chosen redundant joint variable.

The configuration space of the manipulator is spanned by the joint variables and it is restricted by the mechanical construction of the robot. Differential constraints, on the other hand, are imposed by the system dynamics, which can be described by the following Euler-Lagrange equation [9]

$$\frac{d}{dt}\left[\frac{\partial \mathcal{L}(q,\dot{q})}{\partial \dot{q}}\right] - \frac{\partial \mathcal{L}(q,\dot{q})}{\partial q} = B(q)u \qquad (4)$$

with the Lagrangian given by $\mathcal{L}(q,\dot{q}) = K(q,\dot{q}) - V(q)$, where $K(q,\dot{q})$ represents the kinetic energy of the system, $V(q)$ is the potential energy, and $B(q)u$ forms the vector of external and controlled forces and torques. For a hydraulically powered crane, velocity constraints show up naturally due to a maximum flow rate through the hydraulic system, whereas acceleration constraints are given through maximum producible forces and torques of the hydraulic actuators. Differential constraints are typically configuration dependent.

In this study we will only use configuration and velocity constraints as given in Table II. Procedures for computing

TABLE II
Position and velocity constraints of the 4-link manipulator

Link i	$q_{i,\min}$	$q_{i,\max}$	$\dot{q}_{i,\min}$	$\dot{q}_{i,\max}$
1	-3 rad	3 rad	-0.8 rad/s	0.8 rad/s
2	-0.4 rad	1.5 rad	-0.5 rad/s	0.5 rad/s
3	-3 rad	-0.15 rad	-0.8 rad/s	0.8 rad/s
4	0	3.5 m	-1.2 m/s	1.2 m/s

reliable estimates of dynamical parameters as well as obtaining accurate quantitative description of external forces in (4) are currently under study. The range of allowable velocities is taken as an average of frequently encountered minimum

and maximum velocities along numerous human-operated motions. Even though the operator was a very experienced professional, this measure does not reflect the full potential of the machine and should be therefore understood as a conservative figure.

III. Recording the Human-Operated Process

Forwarder cranes are used to collect logs from the ground to the tray for transportation out of the harvesting area. In order to take measurements of the real process, various sensors are installed at the crane, wired to a processing unit. We used a dSPACE 1401 real-time prototyping platform for data streaming to a connected laptop capturing the joint variables q from high-resolution encoders manufactured by Heidenhain. The sampling time was $0.01\,\mathrm{s}$. Velocity estimates are obtained by applying a simple discrete-time differentiater to the position signals after noise was removed by zero-phase digital filtering.

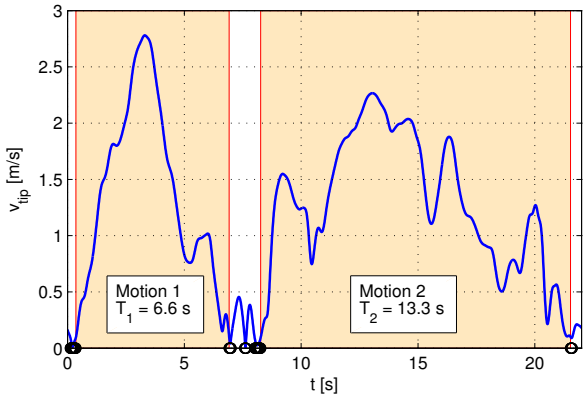

Fig. 3. Absolute boom-tip velocity during a time interval containing two types of motions: (1) motion from the tray towards logs, and (2) motion with logs in the end effector back to the tray.

In order to select relevant motions of the process we looked at the absolute boom-tip velocity

$$v^0(t) = \left\| \frac{d}{dt} p^0(t) \right\| \tag{5}$$

subject to a threshold value of $0.1\,\mathrm{m/s}$. Motions below this value and, additionally, shorter than $3\,\mathrm{s}$ are considered as local grasping tasks of no relevance to this study. In Fig. 3 the absolute boom-tip velocity (5) is shown for a short time interval of the recorded data containing two types of motions. During the *outward motion*, the crane arm is moved away from the tray towards a pile of logs that will be shortly collected. This motion is performed with an empty gripper. The second type of motion, the *inward motion*, is performed after the logs are grasped, when the crane moves the logs back to the tray. Since the inward motions are executed with unknown payload (the weight of the logs), they are harder to analyze if we consider constraints on accelerations imposed by (4). We, therefore, restrict our analysis to the outward motions.

Approximately 15 minutes of continuous normal operation was recorded for the loading process of picking up logs to the tray. During this time, 46 motions are performed, i.e. 23 outward motions that can be analyzed. In Fig. 4 we see the end points for a number of typical motions in a virtual environment developed in [10]. Additionally, the path of the boom tip is shown for one outward motion and its subsequent inward motion.

IV. Analysis of a Human-Operated Motion

In this section we analyze a particular human-operated motion in order to illustrate its parameterization without explicit dependence on time. Let us consider the motion from point A to B in Fig. 4. All configuration variables are recorded with respect to time. Thus, the Cartesian position of the boom tip can be found and computed by using the forward kinematics (2).

Procedure 1: Representation of Motions

1. Define a new variable that describes the path as a function of the generalized coordinates. For instance, the arc length along the path would be one choice that naturally yields a monotonic time evolution:
$$\theta(t) = \int_{t=0}^{T} \left\| \frac{d}{dt} p^0(t) \right\| dt\,. \tag{6}$$
2. All joint variables must be parameterized as function of the new variable θ instead of time:
$$\begin{bmatrix} q_1 \\ q_2 \\ q_3 \\ q_4 \end{bmatrix} := \Phi(\theta) = \begin{bmatrix} \phi_1(\theta) \\ \phi_2(\theta) \\ \phi_3(\theta) \\ \phi_4(\theta) \end{bmatrix}. \tag{7}$$
It can be understood as synchronization of all joints along the path clocked to the independent configuration variable θ.

With such a representation the explicit dependence on time of the generalized coordinates is removed, whereas the path coordinate $\theta(t)$ can be viewed as a motion generator for the specified path. Once a velocity profile for θ is chosen—it might be assigned different from the recorded one—all joint velocities are directly assigned by

$$\dot{q} = \Phi'(\theta)\dot{\theta}\,, \tag{8}$$

meaning that the nominal evolution of the full state space vector $[q, \dot{q}]^T$ is parameterized along the path without the need of the system dynamics (4). This approach is known as *path-constrained trajectory planning* [5], which is however subject to velocity and acceleration constraints. In the context of control theory, the geometric function (7) is called a *virtual holonomic constraint* [8] if it is preserved by some control action along solutions of the closed-loop system.

In the case of the human-operated motion no differential constraints have to be considered, since the motion was recorded to be feasible. Therefore, we take the time derivative of (6) and map it onto θ. It means that we can directly shape a curve in the $(\theta, \dot{\theta})$-phase plane that assigns velocity profiles along a specified path. However, the differential equation relating θ and $\dot{\theta}$ is subject to the individual joint velocity and acceleration constraints. The

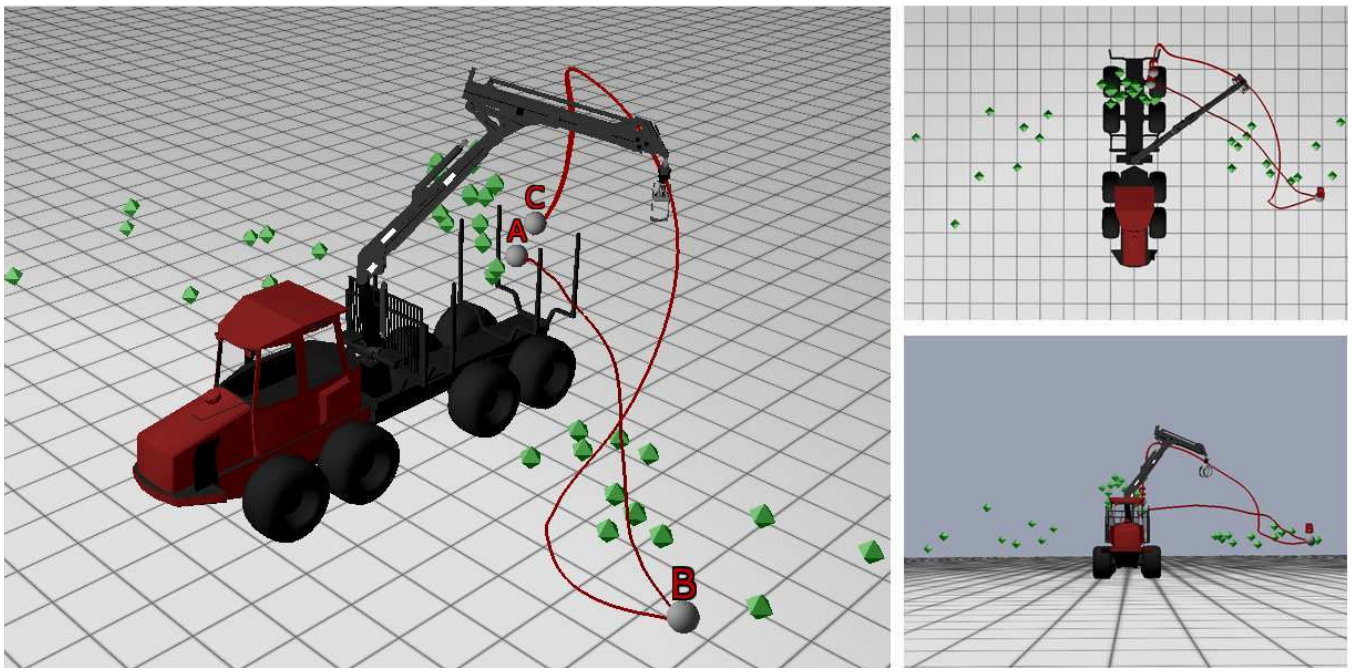

Fig. 4. The forwarder crane and target postions in a virtual environment developed in [10]. Two types of motions are depicted: (1) motion from the tray towards logs along path $\overline{AB}$, and (2) motion with logs in the end effector back to the tray along path $\overline{BC}$.

time evolution of θ along the path is derived by integrating this differential equation, which defines the time evolution of all joint coordinates in (7). As a result, the whole motion of the manipulator along a specified path can be generated following the simple numerical steps introduced above.

Shaping curves in the $(\theta, \dot{\theta})$-phase plane can be instrumental for assignments of different velocity profiles along the same path, such that the human-operated trajectory can be replanned based on optimization for time or other performance measures.

V. Replanning for Path-Constrained Time-Efficient Trajectories

Keeping the joint profiles (7) of the human-operated motion does not allow us to assign much higher velocity profiles compared with the driver due to velocity constraints. However, we can replan the trajectory along the same Cartesian path using different joint profiles since the manipulator is kinematically redundant. The following optimization procedure for trajectories with small execution time is suggested:

Procedure 2: Planning Path-Constrained Time-Efficient Trajectories

1. Parameterize the redundant joint variable $q_4 := \phi_4(\theta)$ by some function, chosen to be a Bézier polynomial [11] of degree $M = 10$, i.e. $\phi_4(\theta) = b_{q_4}(s)$:

$$b_{q_4}(s) = \sum_{k=0}^{M} a_{q_4,k} \frac{M!}{k!(M-k)!} s^k (1-s)^{M-k} \quad \text{where} \quad s = \theta/\theta_{end}\,. \tag{9}$$

2. Apply inverse kinematics (3) to compute the full vector function $\Phi(\theta)$ along the given path.
3. The optimal joint profile (9) is found for the polynomial coefficients $x_{par} = \{a_{q_4,1}, \ldots, a_{q_4,M}\}$ that maximize the area under the envelope function formed by the individual joint velocity constraints along the path using (8). For the numerical search we use `fmincon` from MATLAB such that the inverse kinematics (3) is feasible. The parameter $a_{q_4,0}$ is taken as the initial extension of the telescope. A time-efficient trajectory is finally obtained by constructing a smooth curve in the $(\theta, \dot{\theta})$-phase plane close enough to the velocity constraints without violating them.

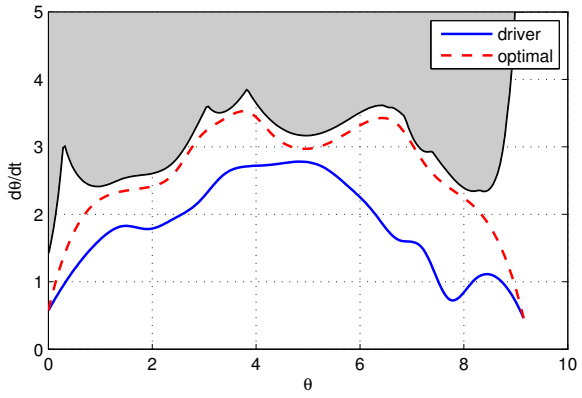

Fig. 5. Velocity profiles along the path in the $(\theta, \dot{\theta})$-phase plane. The path-constrained optimal curve from Procedure 2 yields a faster motion compared with the driver. Velocity constraints along the path are indicated as gray area not to be violated. Velocities at the start and end are non-zero due to the choice of time intervals for relevant motions (see Fig. 3).

Fig. 5 shows the path-constrained optimal trajectory superimposed with velocity constraints projected along the path. The resulting joint trajectories from this optimized solution are shown in Fig. 6. The execution times for a number of

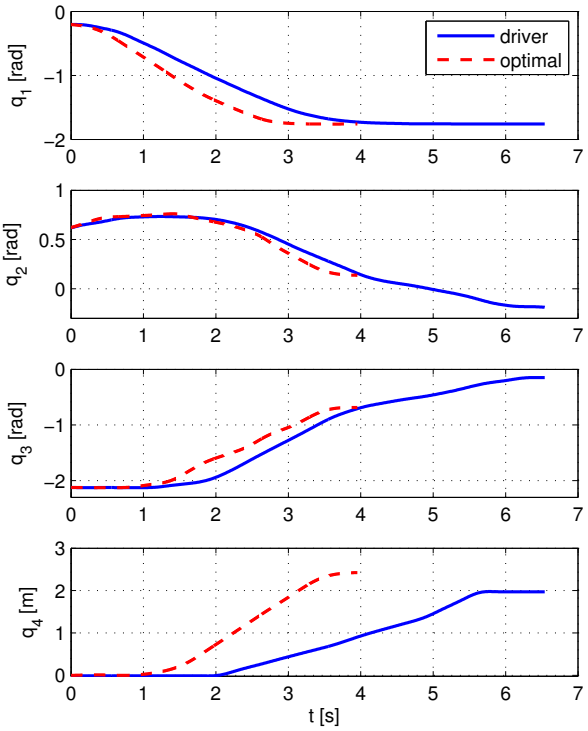

Fig. 6. Evolution of joint coordinates with respect to time. The motion with a time-efficient velocity profile obtained from Procedure 2 is clearly faster than the one of the driver.

TABLE III

EXECUTION TIME FOR HUMAN OPERATOR AND OPTIMIZED TRAJECTORY TOGETHER WITH SPEED IMPROVEMENT FOR DIFFERENT MOTIONS

Motion	T	T_{opt}	Improvement
1	6.54	3.95	1.65
2	7.68	4.94	1.55
3	7.19	6.81	1.05
4	3.94	2.71	1.44
5	5.62	4.28	1.31
6	5.38	3.58	1.49
7	5.12	3.21	1.59
8	6.02	3.90	1.54
9	5.44	4.07	1.33
10	5.12	3.21	1.59
Average	5.81	4.07	1.49

such optimized motions are stated in Table III along with a comparison to the corresponding human-operated motions. In average over ten motions, the speed along the driver's path of the boom tip can be improved by a factor of 1.49 by replanning the trajectories.

We should make clear that Procedure 2 for finding efficient trajectories guarantees that the individual joint velocity constraints are not violated, which is a major advantage compared with methods involving a pseudo-inverse of the end-effector Jacobian commonly used for redundant manipulators (see e.g. [6], [3]). In step 2 the non-uniqueness issue is resolved such that the joint coordinates are continuous functions along the target path.

VI. TRAJECTORY REPLANNING FOR TIME-EFFICIENT PATH AND VELOCITY PROFILE

The proposed approach can be generalized if we consider the problems of searching a time-efficient Cartesian path and a time-efficient velocity profile for a given start and end point of the boom tip simultaneously. The optimization procedure is similar to the one described above, but now we also have to parameterize the Cartesian boom-tip position p^0 by some function, which in turn generates a different path compared to the human-operated motion when getting optimized.

Procedure 3: Planning Trajectories with Time-Efficient Path and Velocity Profile

1. We take again a parameterization as Bézier polynomials (9) of degree $M = 10$ for the Cartesian positions x, y, z and the redundant joint variable q_4:
$$\begin{aligned} p^0(t) &:= [b_x(s), b_y(s), b_z(s)]^T \\ q_4(t) &:= b_{q_4}(s) \\ \text{where} \quad s &= t/1\,, \end{aligned} \tag{10}$$
but now with respect to a virtual time $t \in [0, 1]$.
2. Apply the numerical steps of Procedure 1 for removing the explicit time dependence such that the independent variable θ works like a motion generator through the virtual holonomic constraint.
3. Apply inverse kinematics (3) using (10) to compute the full vector function $\Phi(\theta)$ along the currently specified path.
4. An optimal Cartesian path and optimal joint profiles along this path are found for the polynomial coefficients
$$x_{par} = \{ \quad a_{x,1}, \ldots, a_{x,M-1}, a_{y,1}, \ldots, a_{y,M-1}, \\ a_{z,1}, \ldots, a_{z,M-1}, a_{q_4,1}, \ldots, a_{q_4,M} \quad \}\,,$$
that maximize the area under the envelope function formed by the individual joint velocity constraints using (8) and, at the same time, yield the shortest time for traversing along a newly shaped path. Here, we simply integrate the dynamics constructed in the $(\theta, \dot{\theta})$-phase plane applying `ode45` from MATLAB for each parameter set within the current range of the path coordinate θ, which gives the time to be minimized. For the numerical search we use `fmincon` such that the inverse kinematics (3) is feasible. The parameters $[a_{x,0}, a_{y,0}, a_{z,0}]^T = p^0(t = 0)$ are already given by the initial point and $[a_{x,M}, a_{y,M}, a_{z,M}]^T = p^0(t = 1)$ by the final point; $a_{q_4,0}$ is taken as the initial extension of the telescope.

In Fig. 7 we show the time-efficient path compared with the human-operated path from the same initial point to the same target point. The time-efficient motion is two times faster. As expected, the curves look much smoother in case of the optimal path. In Fig. 8 it is shown that the optimal velocity profile along the new path is much higher compared with the one from the human operator and also compared with the path-constrained optimized velocity profile from Procedure 2. Hence, changing the path of the boom tip and optimizing for performance is a powerful tool for efficient motion planning.

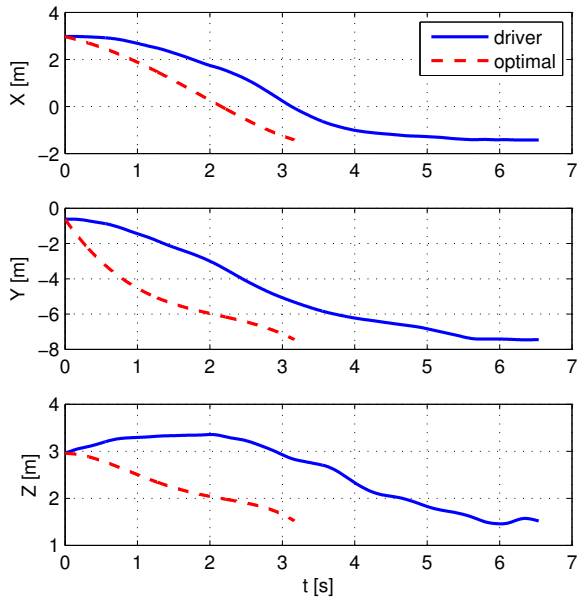

Fig. 7. Evolution of Cartesian position of the boom tip with respect to time. The motion with time-efficient Cartesian path and velocity profile from Procedure 3 is clearly faster than the one of the driver and has a smoother path of the boom tip.

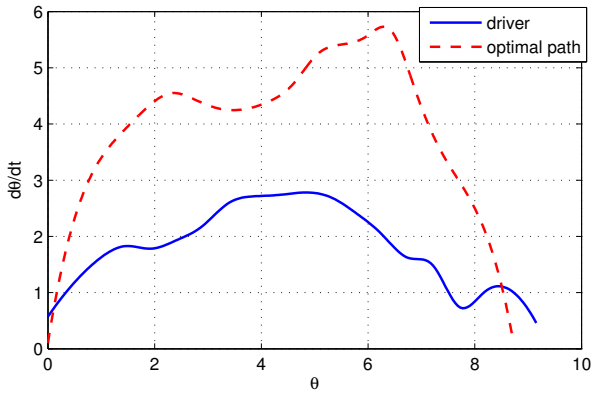

Fig. 8. Velocity profiles along the individual Cartesian paths of the driver and the newly found optimal path from Procedure 3 in the $(\theta, \dot{\theta})$-phase plane. Note that the length along the optimal path $\theta_{\max}$ is smaller compared with the one from the human operator.

VII. Conclusions

In this paper we have considered the problem of trajectory planning for a kinematically redundant manipulator used on forestry machines. In particular, we have analyzed crane trajectories that were recorded from a professional human operator moving the end-effector from the tray towards logs, which is generally executed fastest because no payload has to be taken care of.

An optimization procedure is suggested that takes advantage of the kinematic redundancy so that the configuration of the crane along specified Cartesian paths can be modified giving efficient velocity profiles. Differential constraints imposed by the manipulator dynamics are accounted for by employing a phase-plane technique for admissible path timings. In this study we concentrated on the dominant velocity constraints which are apparent in hydraulic actuators. It is straightforward to also account for acceleration constraints.

The following results have been presented:

- Path-constrained replanning of human-operated motions can speed up the process by a factor of 1.49 in average.
- Trajectory replanning for time-efficient paths and velocity can speed up the process by a factor of 2.

We conclude that smart motion planning and control has a big potential to speed up motions of forestry cranes compared to today's operators. It is important to note that we can also use other quantities such as mechanical power or reaction forces to optimize for, but it requires full knowledge of the system dynamics.

The following semi-autonomous scenario seems realizable in the near future: Fill the working space of the crane with numerous paths to different targets required for the process and have a driver select the target point. An offline/online motion planning strategy together with a controller allows for moving the end effector in an optimal way. Near the target point the driver can take over for the grasping task. An interesting question in such a scenario is the interface of the driver to the automatic control system. We currently study how to use the joysticks and a virtual environment to specify target motions and possibly modify their velocity profiles or shift to nearby trajectories.

References

[1] J. Billingsley, A. Visala, and M. Dunn, *Springer Handbook of Robotics*. Berlin / Heidelberg: Springer-Verlag, 2008, ch. Robotics in Agriculture and Forestry, pp. 1065–1077.

[2] J. Bobrow, S. Dubowsky, and J. Gibson, "Time-optimal control of robotic manipulators along specified paths," *The International Journal of Robotics Research*, vol. 4, no. 3, pp. 3–17, 1985.

[3] S. Chiaverini, G. Oriolo, and I. Walker, *Springer Handbook of Robotics*. Berlin / Heidelberg: Springer-Verlag, 2008, ch. Kinematically Redundant Manipulators, pp. 245–268.

[4] J. Hollerbach, "Dynamic scaling of manipulator trajectories," *ASME Journal of Dynamic Systems, Measurement, and Control*, vol. 106, no. 1, pp. 102–106, 1984.

[5] S. LaValle, *Planning Algorithms*. New York: Cambridge University Press, 2006.

[6] R. Patel and F. Shadpey, *Control of Redundant Robot Manipulators*. Berlin / Heidelberg: Springer-Verlag, 2005.

[7] K. Shin and N. McKay, "Minimum-time control of robotic manipulators with geometric path constraints," *IEEE Transactions on Automatic Control*, vol. 30, no. 6, pp. 531–541, 1985.

[8] A. Shiriaev, J. Perram, and C. Canudas-de-Wit, "Constructive tool for orbital stabilization of underactuated nonlinear systems: Virtual constraints approach," *IEEE Transactions on Automatic Control*, vol. 50, no. 8, pp. 1164–1176, 2005.

[9] M. Spong, S. Hutchinson, and M. Vidyasagar, *Robot Modeling and Control*. New Jersey: John Wiley and Sons, 2006.

[10] S. Westerberg, I. Manchester, U. Mettin, P. La Hera, and A. Shiriaev, "Virtual environment teleoperation of a hydraulic forestry crane," in *Proceedings of the 2008 IEEE International Conference on Robotics and Automation*, Pasadena, USA, May 19-23 2008.

[11] E. Westervelt, J. Grizzle, C. Chevallereau, J. Choi, and B. Morris, *Feedback Control of Dynamic Bipedal Robot Locomotion*. CRC Press, Taylor and Francis Group, 2007.